Available online at www.sciencedirect.com
SCIENCE DIRECT®
Journal of Magnetic Resonance 169 (2004) 1–12
JMR Journal of Magnetic Resonance
www.elsevier.com/locate/jmr

Sensitivity enhancement in pulse EPR distance measurements

G. Jeschke,[a,*] A. Bender,[b] H. Paulsen,[b] H. Zimmermann,[c] and A. Godt[a,d]

[a] *Max Planck Institute for Polymer Research, Postfach 3148, 55021 Mainz, Germany*
[b] *Universität Mainz, Institut für Allgemeine Botanik, Müllerweg 6, 55128 Mainz, Germany*
[c] *Max Planck Institute for Medical Research, Jahnstrase 29, 69120 Heidelberg, Germany*
[d] *Universität Bielefeld, Fakultät für Chemie, Universitätsstrasse 25, 33615 Bielefeld, Germany*

Received 20 January 2004; revised 7 March 2004
Available online 22 April 2004

Abstract

Established pulse EPR approaches to the measurement of small dipole–dipole couplings between electron spins rely on constant-time echo experiments to separate relaxational contributions from dipolar time evolution. This requires a compromise between sensitivity and resolution to be made prior to the measurement, so that optimum data are only obtained if the magnitude of the dipole–dipole coupling is known beforehand to a good approximation. Moreover, the whole dipolar evolution function is measured with relatively low sensitivity. These problems are overcome by a variable-time experiment that achieves suppression of the relaxation contribution by reference deconvolution. Theoretical and experimental results show that this approach leads to significant sensitivity improvements for typical systems and experimental conditions. Further sensitivity improvements or, equivalently, an extension of the accessible distance range can be obtained by matrix deuteration or digital long-pass filtering of the time-domain data. Advantages and limitations of the new variable-time experiment are discussed by comparing it to the established analogous constant-time experiment for measurements of end-to-end distances of 5 and 7.5 nm on rod-like shape-persistent biradicals and for the measurement of a broadly distributed transmembrane distance in a doubly spin-labeled mutant of plant light harvesting complex II.

Keywords: EPR; ELDOR; Spin labeling; Protein structure; Pair correlation function

1. Introduction

Site-selective distance measurements between spin labels or spin probes have recently found increasing application in both life sciences [1–3] and materials sciences [4,5]. Most of these applications are concerned with the characterization of structure and structural dynamics of non-crystalline systems on length scales between 0.5 and 5 nm, for which few alternative techniques exist. Distances in the lower range between 0.5 and 2 nm are best measured by continuous-wave (CW) EPR methods, while the upper range between 2 and 5 nm is the domain of pulse EPR methods [6–13], which have higher resolution and allow for a more detailed characterization of distance distributions [14–16]. This upper range is of particular interest for the characterization of molecular arrangements in biological and synthetic supramolecular assemblies [17–19] and for structure elucidation of biomacromolecules such as soluble proteins [20,21], ribonucleic acids [22], and membrane proteins [23].

Development of EPR methods for such applications should be based on the comparative advantages and disadvantages of EPR with respect to alternative characterization techniques. Compared to scattering techniques, such as small-angle neutron scattering (SANS) [24], EPR distance measurements have higher sensitivity and better site selectivity, while compared to fluorescence resonance energy transfer (FRET) techniques [25] EPR sensitivity is much lower. However, EPR techniques also have several advantages with respect to FRET. First, the molecular size of the probes or labels is significantly smaller, so that the original structure is less perturbed and measurements are potentially more precise. Second, labeling protocols are simpler, as EPR can

* Corresponding author. Fax: +49-6131-379-100.
E-mail address: jeschke@mpip-mainz.mpg.de (G. Jeschke).

1090-7807/$ - see front matter © 2004 Elsevier Inc. All rights reserved.
doi:10.1016/j.jmr.2004.03.024

measure distances between two labels with the same structure, while established FRET techniques require two different chromophores. Third, unlike FRET, EPR is applicable to opaque materials. For many applications, these two spectroscopic methods for the measurement of distances between dipoles may thus provide complementary information. However, there is still a broad range of systems to which neither method can be applied on a routine basis. In the case of pulse EPR, this is mainly due to limitations in sensitivity. While the protein concentrations and amounts of sample required for CW EPR can be routinely achieved for many membrane proteins, pulse EPR is still restricted to proteins that can be produced in large amounts and reconstituted at concentrations that are much higher than in native biomembranes. Increasing concentration sensitivity and absolute sensitivity of such measurements is thus of considerable interest.

In the present work, we reconsider an established design principle of EPR pulse sequences for distance measurements, namely the suppression of relaxational decay contributions to the signal by keeping the total length of the pulse sequence constant. For measurements of distances longer than 3 or 4 nm this principle requires a length of the pulse sequence that significantly exceeds the phase memory time of electron spins in typical systems. Accordingly, the dipolar evolution function is measured as the variation of a very small fraction of the total echo intensity, which leads to sensitivity loss. We examine, whether the alternative approach of a variable-time experiment with reference deconvolution can overcome this problem. For further sensitivity improvement, we consider lengthening of the phase memory time by matrix deuteration and partial noise suppression in data analysis by digital filtering.

The paper is organized as follows. First, we analyze the relation between sensitivity and accessible distance range for a theoretical model that consists of dilute clusters of spins (dilute nanoobjects). This model is applicable, but not restricted, to doubly labeled macromolecules and includes purely decaying contributions to the dipolar evolution function that are caused by the interaction between spins in different clusters. We then consider how the required maximum dipolar evolution time depends on the maximum distance between spins within the same cluster. Second, we examine both theoretically and experimentally, whether a variable-time experiment with reference deconvolution provides the same dipolar evolution function as a constant-time experiment and, whether such an experiment indeed has higher sensitivity. We also consider subtle differences between the variable- and constant-time approaches that arise for a distribution of local structures within the cluster that is correlated to a distribution of relaxation times. Third, we examine deuteration of only the matrix in which the nanoobjects are diluted rather than of the nanoobjects themselves as a means of increasing sensitivity. Finally, we discuss the equivalence of a digital low-pass filter to a long-pass distance filter and the question, whether such a filter can suppress artifacts in a distance range where it does not suppress true peaks in the distance distribution. This question is addressed experimentally on a doubly spin-labeled double mutant of plant light-harvesting complex II with spin-to-spin distances in the range between 3.7 and 5.2 nm.

2. Materials and methods

2.1. Model systems

Synthesis of the shape-persistent biradical with an end-to-end distance of approximately 5 nm has been described earlier [26]. The shape-persistent biradical with an end-to-end distance of approximately 7.5 nm was synthesized in an analogous way. The double mutant S106C/S160Ch of the LHCII apoprotein was dissolved (1 mg/ml) in an aqueous solution of SDS (0.5 wt%) and sodium phosphate buffer of, pH 7 (20 mM). Reduction of any present disulfide linkages to free SH groups was achieved by incubation with Tris-(2-carboxyethyl)phosphine (TCEP, 2 mM) for 2 h. Spin labelling was performed by adding 4-(2-iodoacetamido)-2,2,6,6-tetramethylpiperidine-1-oxyl (Sigma–Aldrich, 10-fold molar excess) and incubating over night at ambient temperature on a shaker. The protein was then precipitated by addition of 100 mM acetic acid (1/10 of the original volume) and acetone (2.3 times the original volume). After centrifugation, the protein was washed several times with 70% ethanol/30% water and once with absolute ethanol. The protein pellet was dried for 15 min at ambient temperature. This doubly labelled protein was then used in reconstitution of LHCII following a standard procedure [27].

2.2. EPR measurements

Dipolar time evolution data were obtained at X-band frequencies (9.3–9.4 GHz) with a Bruker Elexsys 580 spectrometer equipped with a Bruker Flexline split-ring resonator ER 4118X_MS3. Microwave from a YIG oscillator (Avantek AV 78012) customized by Magnettech GmbH Berlin was fed into one microwave pulse forming unit of the spectrometer to provide the pump pulses. All measurements were performed using the four-pulse DEER experiment $\pi/2(\nu_{\mathrm{obs}}) - \tau_1 - \pi(\nu_{\mathrm{obs}}) - t' - \pi\ (\nu_{\mathrm{pump}}) - (\tau_1 + \tau_2 - t') - \pi(\nu_{\mathrm{obs}}) - \tau_2 - \mathit{echo}$ [10]. In the constant-time version, time t' is varied, while τ_1 and τ_2 are kept constant. In the variable-time version, the reference trace is obtained with $t' = \tau_1 = \text{const.}$ by varying τ_2. The recoupled trace is acquired with the same variation of τ_2 and constant τ_1 by incrementing

time t' by the same step as time τ_2 starting at $t'(0) = \tau_1$. The dipolar evolution time is $t = t' - \tau_1$. Data were analyzed only for $t > 0$. The resonator was overcoupled to $Q \approx 100$, the pump frequency ν_{pump} was set to the center of the resonator dip and coincided with the maximum of the nitroxide EPR spectrum, while the observer frequency ν_{obs} was 65 MHz higher and coincided with the low-field local maximum of the spectrum. All measurements were performed at a temperature of 50 K with observer pulse lengths of 32 ns for both $\pi/2$ and π pulses and a pump pulse length of 12 ns. Proton modulation was averaged by adding traces at eight different τ_1 values, starting at $\tau_1(0) = 200$ ns and incrementing by $\Delta t_1 = 8$ ns, except for the deuterated matrix, where $\tau_1(0) = 400$ ns was used, corresponding to a blindspot of the deuterium modulation. In all experiments we used $\tau_2(0) = \tau_1 + 100$ ns which is sufficient to avoid overlap of different echoes and thus obviates the need for additional phase cycling.

2.3. Data analysis

The theoretical model for data analysis is described below. Computation of pair correlation functions (distance distributions) by cubic hermite interpolation between sampling points as described in [16] was accomplished with home-written Matlab programs.

3. Trade-off between sensitivity and distance range

3.1. Oscillatory and purely decaying contributions to the dipolar evolution function

The particular strengths of pulse EPR distance measurements are site selectivity and the possibility to characterize local order in systems that lack long-range order. Such measurements are therefore, often applied to systems that consist of well defined isolated objects with a size between 2 and 10 nm, such as a labeled biomacromolecules [20–23], aggregates of labeled peptides [17], or clusters of ionic endgroups in a polymer [28]. The spatial distribution of the nanoobjects in the sample can often be considered as homogeneous in three dimensions (soluble proteins), two dimensions (membrane proteins), or one dimension (rodlike polymers). For most purposes, it can be described as a homogeneous distribution with fractal dimension $1 \leqslant D \leqslant 3$ and parameter α that is proportional to the density of spins [29]. For $D = 3$, the density corresponds to the bulk concentration. The individual objects can be generally described as clusters with an average number of spins $\overline{n}$, where $\overline{n} = 2$ corresponds to the case of highly diluted spin pairs as, e.g., in doubly labeled proteins. The inner structure of the nanoobjects is characterized by a pair correlation function $G_{\mathrm{cluster}}(r)$, which is normalized

$$\int_{r_{\min}}^{r_{\max}} 4\pi r^2 G_{\mathrm{cluster}}(r)\mathrm{d}r = \overline{n} - 1. \tag{1}$$

Note that this mathematical description is also valid for cases where individual clusters may have different numbers of spins and where their inner structure varies to some extent. In this situation $G_{\mathrm{cluster}}(r)$ corresponds to an average structure.

The dipolar evolution function obtained by pulse ELDOR experiments on a multi-spin system factorizes into pair contributions [7]. Thus, it is possible to derive an analytical expression for the normalized dipolar evolution function obtained by the double electron electron resonance (DEER) experiment on a system conforming to this very general structural model. Using expressions from [14,16], we obtain for the normalized echo signal:

$$\ln V(t) = -\lambda\left\{\overline{n} - 1 + \alpha t^{D/3} - \int_{r_{\min}}^{r_{\max}} 4\pi r^2 G_{\mathrm{cluster}}(r) V_{\mathrm{pair}}(r,t)\mathrm{d}r\right\}, \tag{2}$$

where

$$V_{\mathrm{pair}}(r,t) = \int_0^{\pi/2} \cos\left[\frac{1}{r^3}\frac{\mu_0 g^2 \mu_{\mathrm{B}}^2}{4\pi\hbar}\left(1 - 3\cos^2\theta\right)t\right]\sin\theta\,\mathrm{d}\theta \tag{3}$$

is the dipolar evolution function for a spin pair assuming that there are no constraints on angle θ between the spin–spin vector and the external magnetic field. This assumption corresponds to a macroscopically disordered material and negligible orientation selection [30]. The modulation depth λ is the probability for exciting a spin by the pump pulse, which depends on the kind of paramagnetic center, the excitation bandwidth of the pump pulse, and the excitation position in the spectrum. We assume $\lambda \ll 1$, so that the influence of correlations between more than two spins on the signal is negligible [14]. This relation can be fulfilled by adjusting the length of the pump pulse and thus its excitation bandwidth. The integration limits $r_{\min}$ and $r_{\max}$ in Eqs. (1) and (2) are determined by the excitation bandwidth of the pump pulse and the maximum distance between spins in the cluster, respectively. Typical values for applying a π pump pulse with length between 12 and 32 ns at the maximum of a nitroxide spectrum are $\lambda \approx 0.15$ and $r_{\min} = 1.75$ nm; they depend slightly on the shape of the resonator mode and the detailed structure of the nitroxide label.

Structural characterization of the clusters requires either solving Eq. (2) for $G_{\mathrm{cluster}}(r)$ [14,16] or fitting an appropriate model function for $G_{\mathrm{cluster}}(r)$ by minimizing the least squares deviation between the normalized experimental dipolar evolution function $V(t)$ and a function simulated by Eq. (2) [19,28]. Both approaches

amount to a separation of the cluster contribution from the homogeneous background contribution $\exp(-\lambda\alpha t^{D/3})$. The reliability of the extracted $G_{\mathrm{cluster}}(r)$ thus depends on the success of this separation. The separation can be based on two criteria. First, the cluster contribution is oscillatory, i.e., its first derivative has at least one zero-crossing, while the background contribution is a purely decaying function, whose first derivative is negative at all times. Second, the cluster contribution dominates the short-time behavior, as it corresponds to on average shorter distances and higher dipolar frequencies, while the background contribution dominates the long-time behavior. A model-free approach for extracting $G_{\mathrm{cluster}}(r)$ is only feasible if both criteria are fulfilled. This in turn requires that the distance distribution in the cluster is not too broad, as otherwise the cluster contribution would be overdamped and not oscillatory. Furthermore, the dipolar evolution must be observable up to a time $t_{\max}$ that is sufficiently long to ensure that the background contribution dominates in a time window broad enough for a reasonable fit. The appropriate choice for $t_{\max}$ depends on the maximum distance $r_{\max}$ between spins within a cluster as is discussed in the following.

3.2. Choice of the maximum dipolar evolution time

The dipolar evolution function for a well defined distance r is oscillatory with a frequency that corresponds to the singularity of the Pake pattern at $\theta = 90°$ [15]. The oscillation has a significantly larger and more strongly decaying amplitude during its first half-period compared to later times. In other words, the mean value of the evolution function strongly deviates from zero during the first period, whereas it is close to zero for the following periods. As a result, a reliable separation of oscillatory and purely decaying contributions requires that the signal is observed for at least two periods. Observing two periods also allows for an analysis of the damping of the oscillation that stems from a distribution of distances, i.e., an estimate for the width of the distance distribution can be obtained. In this situation, both the mean distance (first moment of the distance distribution) and its standard deviation (square root of the second moment) are well defined by the experimental data. A rough estimate of the mean distance can already be obtained, if one period of the oscillation is observed, as the dipolar evolution function in such a time window can be distinguished from a purely decaying stretched exponential function corresponding to a homogeneous distribution. If $t_{\max}$ corresponds to only one period, separation of the two contributions is only approximate. Furthermore, one cannot expect to obtain reliable information on the width of the distance distribution.

The period of the dipolar oscillation as a function of the distance is given by

$$t_{\mathrm{dip}}(r) = r^3 \frac{4\pi h}{\mu_0 g^2 \mu_{\mathrm{B}}^2} \approx r^3 \times 0.0192\,\mu\mathrm{s\,nm}^{-3}, \tag{4}$$

where the approximation on the right-hand side applies to pairs of nitroxide radicals. Selecting $t_{\max}$ for the established constant-time experiments [6,8–11] involves a compromise between extending distance range and resolution on the one hand and increasing the signal-to-noise ratio (SNR) of the dipolar evolution function on the other hand, as in all these experiments the function is measured as a variation of an echo signal that is damped by transverse electron spin relaxation during a time of approximately $2t_{\max}$. Our practical experience with four-pulse DEER suggests that for a concentration of spin pairs of 100 μM a sufficient SNR can be obtained within a few hours if the echo amplitude at $t_{\max}$ is at least a few percent of the echo amplitude at $t = 200$ ns. For membrane proteins in an environment of lipids this implies $t_{\max} < 2.5$ μs at the optimum temperature of 50 K. Mean distances and widths of the distance distribution can thus be reliably estimated up to distances of 4 nm, while rough distance estimates are feasible up to distances of 5 nm. In matrices such as *o*-terphenyl, which do not contain methyl groups or highly mobile protons, $t_{\max}$ up to 6 μs may well be feasible. Mean distances and widths can then be characterized for a range up to 5.4 nm, while distance estimates are feasible up to 6.8 nm. Extending this range or increasing SNR by using a deuterated matrix is discussed in a later section.

4. Variable-time four-pulse DEER with reference deconvolution

4.1. Timing of the variable-time four-pulse DEER experiment

The measurement of dipolar time evolution functions with high fidelity requires separation of the coherent evolution of the spin system under the spin Hamiltonian from the incoherent decay due to transverse relaxation. In the established experimental techniques [6,8–11], this is achieved by keeping the total duration of the pulse sequence constant and changing only the timing of individual pulses within the sequence (constant-time experiment). For ELDOR techniques with only a single pump pulse [6,10], relaxation behavior is virtually unchanged for different timings of the pump pulse, so that for practical purposes deconvolution of dipolar evolution and relaxation is complete. Single-frequency techniques [8,9,11] involve a more intricate mixing of the transitions in the two-spin system. It has been pointed out that in this situation a constant-time approach does not fully suppress the relaxational contribution if transverse electron spin relaxation is non-exponential [21].

For optimizing sensitivity, constant-time experiments have two disadvantages. First, the whole dipolar evolution function is measured with a SNR that corresponds to time t_{max}, whereas the function at earlier times could in principle be measured with a shorter pulse sequence and thus with better SNR. Second, t_{max} has to be selected before the measurement, i.e., in a situation where r_{max} may be unknown. For doubly labeled membrane proteins with unknown structure this usually means that for each new double mutant one or more preliminary measurements must be performed before the optimum t_{max} can be selected.

It might appear that the disadvantages can be overcome by measuring portions of the data with different constant duration of the pulse sequence and joining them together. That way earlier parts could be measured with shorter total duration and thus with better signal-to-noise ratio. However, joining the signals together requires a normalization of their respective intensities. The normalization factors have to be determined from the experimental data and are thus subject to an error due to noise. Erroneous normalization factors distort the *shape* of the dipolar evolution function and may thus introduce sizable artifacts into the distance distribution. Therefore, this simple procedure does not work in those cases where it would be most necessary, namely for data with low signal-to-noise ratio.

The two disadvantages can also be avoided by reference deconvolution, which involves the measurement of two signal traces. For the reference trace, the dipole–dipole coupling is not reintroduced, so that the variation of the signal is solely due to relaxation. The second, recoupled trace is measured with a pulse sequence that provides the same relaxational contribution and additionally reintroduces the dipole–dipole coupling. Dividing the recoupled trace by the reference trace yields the pure dipolar evolution function. Normalization of the dipolar evolution function to unity at time zero is inherent in this approach and is thus *exact*, while the normalization factor has to be determined from noisy experimental data in the constant-time approach. This constitutes an additional advantage of reference deconvolution.

Such reference deconvolution is popular in heteronuclear NMR experiments such as REDOR [31], where the reference trace can be obtained by simply skipping the pump pulses. It has also been applied in homonuclear double-quantum NMR experiments [32], where the reference trace corresponds to a different phase cycling than the recoupled trace. Although pulse ELDOR approaches are in principle analogous to heteronuclear NMR experiments and single-frequency EPR approaches to homonuclear NMR experiments, these ideas cannot simply be copied. The phase cycling approach may fail since in contrast to the NMR case, part of the magnetization is lost in EPR as the excitation bandwidth is of the order of the width of the spectrum. Skipping the pump pulse has been suggested for a variable-time field-step ELDOR experiment based on a stimulated-echo sequence [12,13]. Apart from the fact that using a stimulated echo rather than a primary echo entails a loss in signal-to-noise ratio by a factor of two [33], this approach also introduces an additional error into the dipolar evolution function. This is because the pump pulse affects the echo at the observer frequency also in a way that does not depend on dipole–dipole coupling between pumped and observed spins. We usually observe both a phase shift and a small intensity drop, which can be explained by the non-negligible overlap of the excitation bands of the observer and pump pulses.

This problem can be solved by applying the pump pulse in both the reference and recoupled experiments, but timing it differently. This is illustrated in Fig. 1. For the reference trace the pump pulse is always applied at time $2\tau_1$, coinciding with the first echo. This corresponds to dipolar evolution time $t = 0$. By incrementing time τ_2, the purely relaxational echo decay is measured. In the recoupled trace, the pump pulse coincides with the first echo only for the first data point. Its position and thus the dipolar evolution time t are then incremented together with time τ_2.

4.2. Sensitivity comparison of constant- and variable-time DEER

For a quantitative analysis of the relative sensitivity of constant- and variable-time DEER, we consider experiments with the same t_{max}. For simplicity, we assume monoexponential transverse relaxation with time

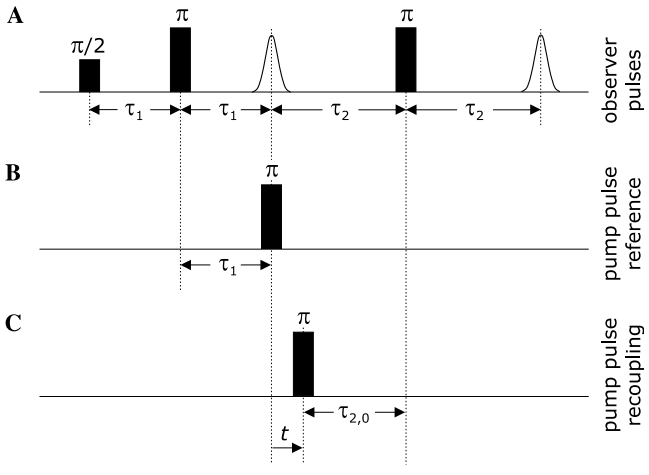

Fig. 1. Pulse timing in variable-time four-pulse DEER. (A) Observer pulses. Time τ_2 is incremented. (B) Pump pulse for the reference trace. The delay with respect to the second observer pulse is fixed, the pump pulse position is not incremented. (C) Pump pulse for the recoupled trace. The delay $\tau_{2,0}$ between the pump pulse and the third observer pulse is constant.

constant T_m. Note, however that the following considerations can be adapted to a different model of relaxation. For the purpose of this discussion, we define the phase memory time T_m in a way that it includes contributions by instantaneous diffusion. Let n be the number of signal accumulations and a_{noise} the noise amplitude of the reference and recoupled trace in the variable-time experiment, while V_0 is the echo amplitude at $t = 0$. In the same measurement time, $2n$ accumulations of the constant-time DEER experiment can be performed, so that the noise amplitude is $\sqrt{2}a_{noise}$ and the signal amplitude is $2V_0$ for this experiment. The signal at dipolar evolution time t is thus given by

$$V_{ct}(t) = 2V_0\ V(t)e^{-t_{max}/T_m}, \tag{5}$$

where $V(t)$ is the normalized dipolar evolution function. For the signal in the reference trace of the variable-time experiment we have

$$V_{ref}(t) = V_0 e^{-t/T_m}, \tag{6}$$

while the signal in the recoupled trace is given by

$$V_{rec}(t) = V_0\ V(t)e^{-t/T_m}. \tag{7}$$

The three signals can be normalized by dividing them by $2V_0$ or V_0, so that the root mean square (r.m.s.) noise amplitudes are given by $\sigma_{vt} = a_{noise}/V_0$ for the two traces of the variable-time experiment and by $\sigma_{ct} = \sqrt{2}\sigma_{vt}/2$ for the constant-time experiment. For the r.m.s. noise amplitude σ_z of the ratio $z = a/b$ of two signals a and b with $\sigma_a = \sigma_b = \sigma_{vt}$, we have

$$\sigma_z = \frac{\sigma_{vt}}{b}\sqrt{1+\frac{a^2}{b^2}}. \tag{8}$$

Substituting $a = V_{rec}/V_0$ and $b = V_{ref}/V_0$, we find

$$\sigma_z(t) = \sigma_{vt}e^{t/T_m}\sqrt{1+V^2(t)}. \tag{9}$$

As expected, the noise amplitude is time-dependent for the variable-time DEER experiment. A measure for the SNR in frequency domain can be obtained by integrating Eq. (9) from $t = 0$ to $t = t_{max}$, as Fourier transformation is a linear integral transformation and we assume white noise. The result depends on the distance distribution. To compute an upper limit for the noise amplitude in frequency domain σ^v_{vt}, we note that $V^2(t) \leqslant 1$ at all times, as $V(t)$ is normalized. We thus obtain

$$\sigma^v_{vt} \leqslant \sqrt{2}\sigma_{vt}T_m\left(e^{t_{max}/T_m} - 1\right). \tag{10}$$

The analogous integration for the constant-time experiment gives

$$\sigma^v_{ct} = \sqrt{2}\sigma_{vt}t_{max}/2. \tag{11}$$

Except for the scaling factor of $\exp(-t_{max}/T_m)$ in the constant-time experiment, the dipolar spectra of both experiments are the same, namely the Fourier transform of $V(t)$. We can thus express the relative SNR by

$$\frac{(S/N)_{vt}}{(S/N)_{ct}} = \frac{\sigma^v_{ct}}{\sigma^v_{vt}e^{-t_{max}/T_m}} \geqslant \frac{t_{max}}{2T_m(1-e^{-t_{max}/T_m})}. \tag{12}$$

This expression is larger than unity for $t_{max} \geqslant 1.6\ T_m$. Hence, in all practically relevant situations, the frequency-domain SNR is higher for the variable-time DEER experiment than for the established constant-time DEER experiment.

The SNR after extraction of $G_{cluster}$ from the time-domain signal is more complicated to predict, as this kind of data analysis is not a linear operation. For fitting a model distance distribution by minimizing the r.m.s. deviation between simulated and experimental time-domain data, all considerations above are valid as well, since this deviation is proportional to the integral of the noise amplitude in the same time window. However, in direct transformation of the time-domain data to a distance distribution the data are scaled by time t before a linear integral transformation and crosstalk correction are applied [14]. An analogous derivation shows that in this situation, the variable-time approach gives better SNR for $t_{max} \geqslant 2.6\ T_m$. This ratio of $t_{max} = 2.6\ T_m$ can be considered as an upper limit of t_{max} at which the constant-time approach can still be competitive with respect to sensitivity. Any smoothing of the distance distribution, which is also inherent in regularization approaches [16], again deemphasizes the contributions to the time-domain signal at later time. We may thus estimate that, irrespective of the type of data analysis, for measurements of distances larger than 3 nm variable-time DEER is expected to be more sensitive than constant-time DEER, as $t_{max} > 2.6\ T_m$ is usually required.

To test these considerations experimentally, we have performed variable-time and constant-time DEER experiments under otherwise identical conditions ($T = 50$ K, width of all observer pulses 32 ns, width of the pump pulse 12 ns, $n = 1500$ averages) on a shape-persistent biradical with an end-to-end distance of approximately 5 nm [26] in glassy *o*-terphenyl. All measurements in this work were performed at X-band frequencies between 9.2 and 9.5 GHz with the same setup and excitation positions as described in our recent work [16,19]. Indeed, the SNR in the variable-time DEER experiment (upper trace in Fig. 2B) is significantly better than in the constant-time experiment (lower trace) at short times and only slightly worse at times close to t_{max}. Accordingly, the SNR in frequency domain (Fig. 2C) is higher for the variable-time experiment (SNR = 496) than for the constant-time experiment (SNR = 126). The SNR enhancement cannot be directly compared with the estimate of Eq. (12), as relaxation is not purely monoexponential. However, we may further approximate that the enhancement factor should be at least $-\ln(f)/2$, where f is the fraction to which the echo signal has decayed by relaxation during time t_{max}. By analyzing the reference trace of the variable-time

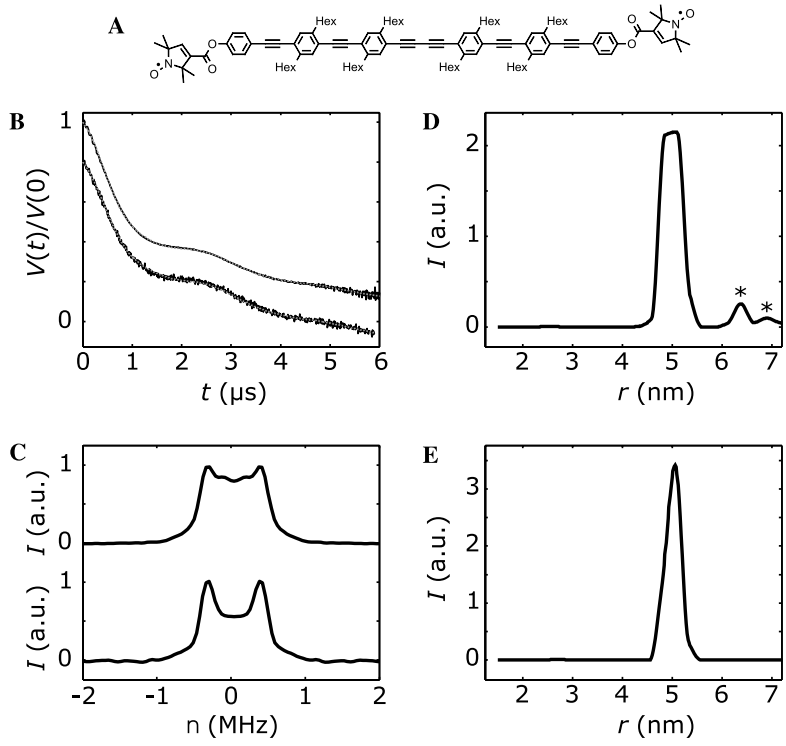

Fig. 2. Four-pulse DEER measurements on a shape-persistent biradical in glassy *o*-terphenyl. (A) Structure of the biradical. (B) Experimental data (black solid lines) of the variable-time experiment (upper trace, $\tau_1 = 200$ ns, $\tau_{2,0} = 300$ ns) and the constant-time experiment (lower trace, normalized, $\tau_1 = 200$ ns, $\tau_2 = 6\,\mu$s). The upper trace is the ratio of the recoupled and reference data, the lower trace has been shifted by −0.2 for clarity. Fits corresponding to the distance distributions in (D) and (E) are shown as superimposed gray dotted lines. (C) Dipolar spectra obtained by Fourier transformation of the data in (B) after exponential background correction. The upper spectrum with a signal-to-noise ratio (SNR) of 495 corresponds to the variable-time experiment, the lower trace with an SNR of 126 to the constant-time experiment. (D) Distance distribution obtained from the variable-time DEER data (65 fitted sampling points between 1.75 and 10 nm, interpolation by Hermite polynomials). (E) Distance distribution obtained from the constant-time DEER data by the same data analysis procedure.

experiment (data not shown) we find $f = 0.012$ and thus predict an SNR enhancement by a factor of at least 2.2. As expected, the experimental enhancement of 3.9 is somewhat higher.

Note also that selecting a shorter $t_{\max}$ in *data analysis* than in the actual measurement leads to an improvement of the SNR for the variable-time experiment, as the part of the time-domain data with lowest SNR is thus excluded from analysis. In contrast, for the constant-time experiment the choice of the *experimental* $t_{\max}$ determines the SNR of the dipolar evolution function at all times, so that the experiment has to be repeated with shorter $t_{\max}$ to achieve an equivalent improvement.

The two dipolar evolution functions are very similar, but closer inspection shows that they are not exactly superimposable, in particular, not for $t \approx t_{\max}$. This is also the reason for the differences in the two dipolar spectra in the vicinity of $\nu = 0$ and for the appearance of small artifacts at 6.3 and 6.9 nm in the distance distribution (asterisks in Fig. 2D) extracted from the variable-time DEER data by the model-free iterative fitting approach introduced in [16]. Such differences between the dipolar evolution functions are not predicted by the theoretical description introduced above. In the following, we discuss how these differences can arise.

4.3. Non-exponential relaxation and selection of subensembles of local structures

Our experience suggests that transverse electron spin relaxation is significantly non-exponential for most samples involving nitroxide spin labels or spin probes. Such non-exponential relaxation corresponds to a distribution of relaxation times T_m. We may also expect that in most systems, there is a distribution of the G_{cluster}, i.e., the distance distribution around the observer spin is not exactly the same for all observer spins. If and only if, the distributions of T_m and G_{cluster} are uncorrelated, we may average them separately. All the expressions derived above, are good approximations for the averages and the measured $V(t)$ should be the same in both experiments. However, G_{cluster} is related to the local structure, and local structure generally influences T_m. In fact, part of the decay in the reference experiment is due to instantaneous diffusion, and that part is certainly correlated to G_{cluster}. Hence, contributions of

observer spins from environments with shorter T_m are partially suppressed at long evolution times t, while contributions from environments with longer T_m are enhanced. The constant-time DEER experiment thus involves a different averaging over the ensemble of local structures than the variable-time DEER experiment. Indeed, in variable-time DEER, the weighting function in the averaging over this ensemble is different at different times t. This may constitute a disadvantage of the experiment, as the mathematical form of $V(t)$ may slightly deviate from the theoretically expected form for a well defined average G_{cluster}.

To test whether this effect is significant, we used a sample for which the functional form of $V(t)$ can be exactly predicted and is well reproduced by a constant-time DEER experiment, namely a solution of nitroxide radicals in a glassy frozen solvent. For such a homogeneous distribution, $V(t)$ has the form of an exponential decay with the decay constant being proportional to the bulk concentration. The arrangement of other nitroxide radicals around an observer radical is different for different observer radicals, and non-exponential transverse relaxation is observed. To obtain a strong effect, we use a solution with bulk concentration of 2 mM, which is much larger than typical concentrations in application-oriented work, and observe the signal up to a time $t_{\max}$ at which $V(t)$ has decayed to approximately 0.2. We find that constant-time DEER data for such a sample are perfectly fit by an exponential decay (gray dotted linear fit function in the lower trace of the logarithmic plot in Fig. 3). In contrast, there is a significant, though not very strong deviation of the fit from the experimental data in the variable-time DEER experiment (upper trace). The deviation is not primarily caused by the residual proton modulation, which is stronger in the variable-time DEER experiment at $t < 1\,\mu s$. Rather, the decay is faster than average at short times t and slower than average at long times t, which agrees with the expectation that differential relaxation selects a subensemble with slower decay at later times.

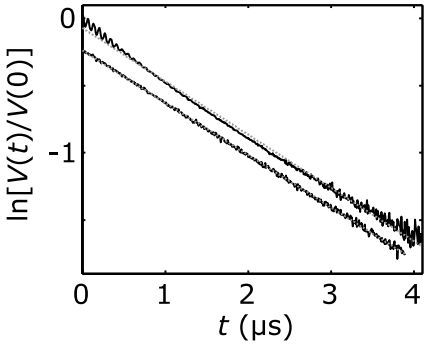

Fig. 3. Four-pulse DEER measurements on an approximately 2.5 mM solution of TEMPOL in glassy toluene (semilogarithmic plot). Experimental data (black solid lines) of the variable-time experiment (upper trace, $\tau_1 = 200\,\text{ns}$, $\tau_{2,0} = 300\,\text{ns}$) and the constant-time experiment (lower trace, normalized, $\tau_1 = 200\,\text{ns}$, $\tau_2 = 4\,\mu s$) are superimposed by linear fits corresponding to exponential decay of $V(t)$ (gray dotted lines). The fast oscillations at short t in the upper trace are residual proton modulations.

Quantitative analysis reveals that the difference is hardly relevant for determination of the bulk concentration. The measurement was performed on a solution with a concentration of 2 mM at room temperature. Toluene shrinks to approximately 80% of its room-temperature volume during shock-freezing in liquid nitrogen, so that the concentration under measurement conditions is approximately 2.5 mM. Earlier calibration experiments gave $\lambda = 0.16$ for the conditions used in this experiment. By inserting the decay time constant (negative slope of the linear fits) into an expression from [15], we find experimental concentrations of 2.44 mM for the constant-time and 2.49 mM for the variable-time DEER experiment. The differences are within experimental error, which is determined mainly by the uncertainty for the volume change of toluene on shock-freezing. This result indicates that differences in $V(t)$ between variable- and constant-time DEER may be significant and may influence the estimated $G_{\text{cluster}}(r)$ at the longest distances, but that they are not dramatic even under conditions that are much less favorable than in most application work. Since extraction of the distance distribution is an ill-posed problem and thus more than linearly dependent on SNR, we anticipate that the gain in SNR is more important for obtaining reliable estimates of G_{cluster} than the slight distortions introduced by time-dependent selection of structural subensembles.

5. Matrix deuteration

From the considerations above, it is clear that T_m is the main determinant of sensitivity that can be influenced by the choice of measurement conditions. At sufficient low temperatures and concentrations [15], the main relaxation mechanism for the electron spins is related to proton spin diffusion. In this situation, T_m can be lengthened by a judicious choice of the solvent. If possible, solvents with methyl groups or other highly dynamic protons should be avoided [34]. A further lengthening of T_m can be obtained by using deuterated solvents as a matrix.

In our attempts to measure the end-to-end distance distribution for a shape-persistent rod-like biradical, with a length of approximately 7.5 nm (Fig. 4A), such matrix deuteration proved crucial. With protonated glassy *o*-terphenyl as a solvent, we could not extend $t_{\max}$ beyond 6 μs corresponding to less than a full oscillation for that distance. With a glassy solution of the protonated biradical in perdeuterated *o*-terphenyl the dipolar evolution could be observed up to $t_{\max} = 24\,\mu s$ with both the variable- and constant-time DEER experiments at

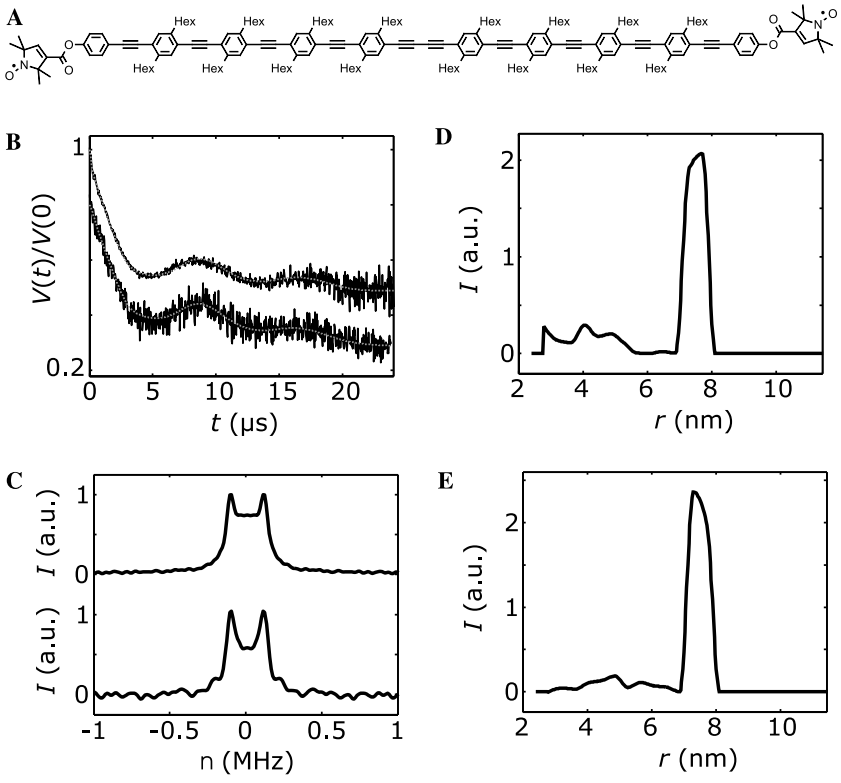

Fig. 4. Four-pulse DEER measurements on a shape-persistent biradical in perdeuterated glassy *o*-terphenyl. (A) Structure of the biradical. (B) Experimental data (black solid lines) of the variable-time experiment (upper trace, $\tau_1 = 400$ ns, $\tau_{2,0} = 500$ ns) and the constant-time experiment (lower trace, normalized, $\tau_1 = 400$ ns, $\tau_2 = 24$ μs). The upper trace is the ratio of the recoupled and reference data, the lower trace has been shifted by −0.2 for clarity. Fits corresponding to the distance distributions in (D) and (E) are shown as superimposed gray dotted lines. (C) Dipolar spectra obtained by Fourier transformation of the data in (B) after exponential background correction. The upper spectrum with a signal-to-noise ratio (SNR) of 137 corresponds to the variable-time experiment, the lower trace with an SNR of 43 to the constant-time experiment. (D) Distance distribution obtained from the variable-time DEER data (65 fitted sampling points between 2.8 and 15.9 nm, interpolation by Hermite polynomials). (E) Distance distribution obtained from the constant-time DEER data by the same data analysis procedure.

50 K (Fig. 4B). This corresponds to approximately three periods of the dipolar oscillation, so that a good estimate of the width of the distribution can be obtained. With the variable-time DEER experiment, we find a mean distance of $\bar{r} = 7.49$ nm and a full width at half height of $\sigma_r = 0.82$ nm (Fig. 4D), while the constant-time experiment gives $\bar{r} = 7.44$ nm and $\sigma_r = 0.82$ nm (Fig. 4E). Again, the SNR of the dipolar spectrum is significantly higher for the variable-time experiment (SNR = 137) than for the constant-time experiment (SNR = 43). This enhancement by a factor of 3.2 is also again larger than the predicted minimum enhancement of $-\ln(f)/2 = 1.33$ for $f = 0.07$. In the normalized time-domain data, the noise amplitude in the variable-time experiment is smaller for at least two periods of the oscillation, so that we may expect that the mean distance and width obtained from this experiment are more precise. We again find that the two dipolar evolution functions are not exactly superimposable at times $t \approx t_{\max}$.

As an additional advantage of matrix deuteration, we find that proton modulation at short t, which is apparent in both Fig. 2B and 3 for the variable-time experiment, is completely suppressed. Deuterium modulation does not occur, i.e., no peak at the deuterium Zeeman frequency of 2 MHz is found in the spectra obtained by Fourier transformation (frequency range not shown). This supports our earlier suggestion that the nuclear modulations are generated by excitation of forbidden transitions of the observer spins by the pump pulse [10]. For smaller Zeeman frequencies, these transitions are closer to the allowed transitions (observer frequency), and thus have a larger offset from the pump frequency. Accordingly, they are to a lesser extent excited by the pump pulse.

The shape-persistent biradicals used so far are virtually ideal model systems for testing range and precision of distance measurements [26] or verifying data analysis procedures for the extraction of distance distributions [14–16]. However, they are not good models for the broader distance distributions that are often encountered in work on biomacromolecules [21], in particular, when labels are situated in loop regions of membrane proteins [16,23]. For membrane proteins, sensitivity problems are usually more serious than for synthetic materials, as sample amounts and bulk concentrations are more difficult to optimize and transverse electron

spin relaxation is faster in lipid/water environments. Due to the complex protocols for reconstitution of membrane proteins and the cost of perdeuterated lipids, matrix deuteration may not be feasible for routine work. As the spin-to-spin distance should ideally be much larger than uncertainties introduced by the size of the labels and their conformational freedom [21], it is furthermore necessary to develop a methodology for measuring distances beyond 3 nm in such samples. To characterize transmembrane distances, the range should be extended to at least 5 nm. At the current stage of development, these requirements are still hard to fulfill on a routine basis. In the following, we therefore, examine the question, whether mathematical noise suppression techniques in data analysis, such as digital filtering, can lead to significant sensitivity improvements for this class of samples. Digital filtering can also be used to suppress nuclear modulation from matrix protons, which appears to be a more serious problem in the presence of water, which forms hydrogen bonds with nitroxides. As a model system, we use the doubly spin-labeled double mutant S106C/S160Ch of light-harvesting complex II, which features spin labels in loop regions on opposite sides of the membrane (Fig. 5A).

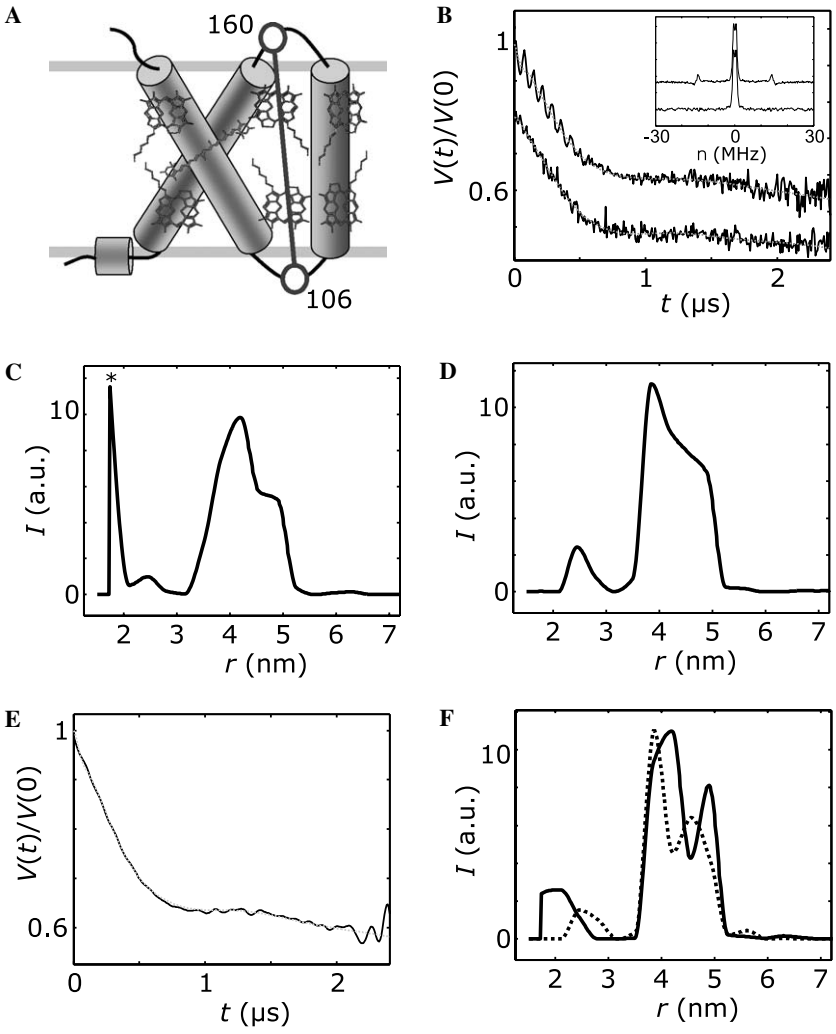

Fig. 5. Four-pulse DEER measurements and digital filtering applied to the doubly spin-labeled double mutant S106C/S160Ch of light-harvesting complex II. (A) Schematic structure of LHCII based on work by Kühlbrandt et al. [35]. The labeling positions are marked by open circles and the spin–spin vector is symbolized by the bold line. (B) Experimental data (black solid lines) of the variable-time experiment (upper trace, $\tau_1 = 200$ ns, $\tau_{2,0} = 300$ ns) and the constant-time experiment (lower trace, normalized, $\tau_1 = 200$ ns, $\tau_2 = 2.5$ μs). The upper trace is the ratio of the recoupled and reference data, the lower trace has been shifted by −0.2 for clarity. Fits corresponding to the distance distributions in (C) and (D) are shown as superimposed gray dotted lines. The corresponding dipolar spectra are shown in the inset. (C) Distance distribution obtained from the variable-time DEER data (17 fitted sampling points between 1.75 and 7.35 nm, interpolation by Hermite polynomials). (D) Distance distribution obtained from the constant-time DEER data by the same data analysis procedure. (E) Time-domain data of the variable-time DEER experiment after digital long-pass filtering with a lower distance cut-off of 1.75 nm. (F) Distance distributions obtained from long-pass filtered variable-time (solid line) and constant-time (dotted line) DEER data.

6. Long-pass digital filtering

6.1. The relation of a low-pass frequency filter to a long-pass distance filter

Pulse EPR experiments for the measurement of distances require that at least one pulse can simultaneously excite two transitions whose frequencies differ by the dipole–dipole coupling [36]. In ELDOR approaches, such as four-pulse DEER, this requirement applies to the pump pulse. The excitation bandwidth of the pump pulse thus imposes an upper limit on the dipolar frequencies that are observable, which translates into a lower limit $r_{\min}$ for the distances that can be measured. Experimental work by several groups suggests that the limit lies between 1.5 and 1.75 nm for pump pulse lengths between 12 and 32 ns [20,37,38], corresponding to a frequency cut-off between 10 and 15 MHz for the splitting between the singularities of the Pake pattern. Though it may in principle be possible to access shorter distances in exceptional cases, we consider it good practice to restrict extraction of distance *distributions* from DEER data to the range above 1.75 nm, as contributions from shorter distances are certainly underweighted. Furthermore, proton modulations introduce an artifact corresponding to approximately 1.5 nm in measurements at X-band frequencies. It is therefore advisable to characterize the range up to 1.75 nm by CW EPR measurements [2,3,39]. If we impose a cut-off toward short distances at 1.75 nm, we can assume that frequencies larger than 10 MHz do not contain information that is of interest in our data analysis. Suppression of these frequencies by a digital low-pass filter should thus not cause any distortions in the distance distribution. Such filtering may improve the appearance of the time-domain data, as is apparent in Fig. 5B and E, so that the low-frequency oscillations may be more easily recognized by visual inspection. It is not immediately clear, however, whether this also improves the extracted distance distribution. This question is addressed in the following.

6.2. Manifestation of time-domain white noise in distance distributions

Extracting the distance distribution from the dipolar evolution function is an ill-posed problem that does not correspond to a linear integral transform. While a distance longer than 1.75 nm certainly cannot contribute a frequency of the singularities of the Pake pattern larger than 10 MHz, noise at frequencies larger than 10 MHz can contribute to artifacts in the distribution at distances longer than 1.75 nm. The reason for this is crosstalk between different frequency channels in the transformation of dipolar evolution functions to the distribution of dipolar frequencies [14]. The crosstalk in turn results from the fact that dipolar evolution functions corresponding to different distances are not orthogonal. High-frequency white noise and proton modulations may thus introduce artifacts into the distance distribution in the range of interest, so that suppression of these contributions before data analysis is advantageous.

Indeed, we find that distance distributions extracted from variable-time DEER data without and with long-pass digital filtering (Fig. 5C and F) are different also in the range above 1.75 nm. The most prominent difference is the partial suppression of the artifact at the lower edge of the distance range (asterisk in Fig. 5C) that stems from the proton modulation. However, filtering also leads to an apparent increase in resolution for the peaks between 3.7 and 5.2 nm, which we find as well for the data from the constant-time experiment (dotted line in Fig. 5F). Likewise, the relative intensity of the artifact at 2.5 nm in the result of the constant-time experiment is slightly decreased by long-pass filtering.

Due to the strong proton modulation at short t, the improvement of the SNR in the variable-time experiment is not easily recognized (Fig. 5B). The SNR in the dipolar spectra (inset) is 125 for the variable-time and 68 for the constant-time experiment. This improvement by a factor of 1.8 is again larger than the predicted minimum improvement of $-\ln(f)/2 = 1.2$ for $f = 0.09$.

7. Conclusion

By merely changing the timing of pulses in the four-pulse DEER experiment and applying reference deconvolution, it is possible to measure the dipolar evolution function with better average signal-to-noise ratio than in the established version of the experiment. This sensitivity improvement leads to a more reliable extraction of distance distributions from experimental data that have been obtained under otherwise identical conditions. Furthermore, the compromise between sensitivity and accessible distance range can be decided during data analysis in the new variable-time approach, while it has to be decided before the measurement in the established constant-time approach. Both approaches were applied to the measurement of a narrowly distributed distance of approximately 7.5 nm in a biradical dissolved in glassy perdeuterated *o*-terphenyl. Digital long-pass filtering of the dipolar evolution function before extraction of the distance distribution can suppress artifacts stemming from nuclear modulations and high-frequency noise, as has been demonstrated on a spin-labeled membrane protein.

References

[1] L.J. Berliner, S.S. Eaton, G.R. Eaton (Eds.), Biological Magnetic Resonance, Vol. 19, Plenum, New York, 2000.

[2] W.L. Hubbell, C. Altenbach, C.M. Hubbell, H.G. Khorana, Trends Biochem. Sci. 27 (2003) 288–295.
[3] H.J. Steinhoff, B. Suess, Methods 29 (2003) 188–195.
[4] A.D. Milov, A.G. Maryasov, Yu.D. Tsvetkov, Appl. Magn. Reson. 15 (1998) 107–143.
[5] G. Jeschke, Macromol. Rapid Commun. 23 (2002) 227–246.
[6] A.D. Milov, K.M. Salikhov, M.D. Shirov, Fiz. Tverd. Tela (Leningrad) 23 (1981) 957–982.
[7] A.D. Milov, A.B. Ponomarev, Yu.D. Tsvetkov, Chem. Phys. Lett. 110 (1984) 67–72.
[8] V.V. Kurshev, A.M. Raitsimring, Yu.D. Tsvetkov, J. Magn. Reson. 81 (1989) 441–454.
[9] P.P. Borbat, J.H. Freed, Chem. Phys. Lett. 313 (1999) 145–154.
[10] M. Pannier, S. Veit, A. Godt, G. Jeschke, H.W. Spiess, J. Magn. Reson. 142 (2000) 331–340.
[11] G. Jeschke, M. Pannier, A. Godt, H.W. Spiess, Chem. Phys. Lett. 331 (2000) 243–252.
[12] L.V. Kulik, Yu.A. Grishin, S.A. Dzuba, I.A. Grigoryev, S.V. Klyatskaya, S.F. Vasilevsky, Yu.D. Tsvetkov, J. Magn. Reson. 157 (2002) 61–68.
[13] A.A. Dubinskii, Yu.A. Grishin, A.N. Savitsky, K. Möbius, Appl. Magn. Reson. 22 (2002) 369–386.
[14] G. Jeschke, A. Koch, U. Jonas, A. Godt, J. Magn. Reson. 155 (2001) 72–82.
[15] G. Jeschke, ChemPhysChem 3 (2002) 927–932.
[16] G. Jeschke, G. Panek, A. Godt, A. Bender, H. Paulsen, Appl. Magn. Reson. 2004 (in press).
[17] A.D. Milov, Y.D. Tsvetkov, E.Y. Gorbunova, L.G. Mustaeva, T.V. Ovchinnikova, J. Raap, Biopolymers 64 (2002) 328–336.
[18] E. Narr, A. Godt, G. Jeschke, Angew. Chem. Int. Ed. 41 (2002) 3907–3910.
[19] G. Jeschke, A. Godt, ChemPhysChem 4 (2003) 1328–1334.
[20] M. Persson, J.R. Harbridge, P. Hammarstrom, R. Mitri, L.-G. Martensson, U. Carlsson, G.R. Eaton, S.S. Eaton, Biophys. J. 80 (2001) 2886–2897.
[21] P.P. Borbat, H.S. Mchaourab, J.H. Freed, J. Am. Chem. Soc. 124 (2002) 5304–5314.
[22] O. Schiemann, A. Weber, T.E. Edwards, T.F. Prisner, S.T. Sigurdsson, J. Am. Chem. Soc. 125 (2003) 3434–3435.
[23] G. Jeschke, C. Wegener, M. Nietschke, H. Jung, H.-J. Steinhoff, Biophys. J. 86 (2004) 2551–2557.
[24] J.S. Higgins, H.C. Benoit, Polymers and Neutron Scattering, Clarendon Press, Oxford, 1994.
[25] P.G. Wu, L. Brand, Anal. Biochem. 218 (1994) 1–13.
[26] A. Godt, C. Franzen, S. Veit, V. Enkelmann, M. Pannier, G. Jeschke, J. Org. Chem. 65 (2000) 7575–7582.
[27] H. Paulsen, B. Finkenzeller, N. Kühlein, Eur. J. Biochem. 215 (1993) 809.
[28] M. Pannier, M. Schöps, V. Schädler, U. Wiesner, G. Jeschke, H.W. Spiess, Macromolecules 34 (2001) 5555–5560.
[29] A.D. Milov, Yu.D. Tsvetkov, Appl. Magn. Reson. 12 (1997) 495–504.
[30] R.G. Larsen, D.J. Singel, J. Chem. Phys. 98 (1993) 5134–5146.
[31] T. Gullion, J. Schaefer, J. Magn. Reson. 81 (1989) 196–200.
[32] T. Dollase, R. Graf, A. Heuer, H.W. Spiess, Macromolecules 34 (2001) 298–309.
[33] A. Schweiger, G. Jeschke, Principles of Pulse Electron Paramagnetic Resonance, Oxford University Press, Oxford, 2001.
[34] M. Lindgren, G.R. Eaton, S.S. Eaton, B.H. Jonsson, P. Hammarstrom, P. Svensson, U. Carlsson, J. Chem. Soc. Perkin Trans. 2 (1997) 2549–2554.
[35] W. Kühlbrandt, D.N. Wang, Y. Fujiyoshi, Nature 367 (1994) 614–621.
[36] In principle, subsequent excitation of the two transitions of the dipolar doublet is also feasible. However, this would introduce a frequency-dependent phase shift and a certain degree of destructive interference.
[37] R.E. Martin, M. Pannier, F. Diederich, V. Gramlich, M. Hubrich, H.W. Spiess, Angew. Chem. Int. Ed. 37 (1998) 2834–2837.
[38] A. Weber, O. Schiemann, B. Bode, T.F. Prisner, J. Magn. Reson. 157 (2002) 277–285.
[39] M.D. Rabenstein, Y.K. Shin, Proc. Natl. Acad. Sci. USA 92 (1995) 8239–8243.